

GenerateCT: Text-Guided 3D Chest CT Generation

Ibrahim Ethem Hamamci^{1*}, Sezgin Er², Enis Simsar³, Alperen Tezcan⁴, Ayse Gulnihane Simsek², Furkan Almas², Sevval Nil Esirgun², Hadrien Reynaud⁵, Sarthak Pati⁶, Christian Blauthgen⁷, Bjoern Menze¹

¹University of Zurich, ²Istanbul Medipol University, ³ETH Zurich, ⁴Ataturk University, ⁵Imperial College London, ⁶University of Pennsylvania, ⁷Stanford University

Abstract

Generative modeling has experienced substantial progress in recent years, particularly in text-to-image and text-to-video synthesis. However, the medical field has not yet fully exploited the potential of large-scale foundational models for synthetic data generation. In this paper, we introduce GenerateCT, the first method for text-conditional computed tomography (CT) generation, addressing the limitations in 3D medical imaging research and making our entire framework open-source. GenerateCT consists of a pre-trained large language model, a transformer-based text-conditional 3D chest CT generation architecture, and a text-conditional spatial super-resolution diffusion model. We also propose CT-ViT, which efficiently compresses CT volumes while preserving auto-regressiveness in-depth, enabling the generation of 3D CT volumes with variable numbers of axial slices. Our experiments demonstrate that GenerateCT can produce realistic, high-resolution, and high-fidelity 3D chest CT volumes consistent with medical language text prompts. We further investigate the potential of GenerateCT by training a model using generated CT volumes for multi-abnormality classification of chest CT volumes. Our contributions provide a valuable foundation for future research in text-conditional 3D medical image generation and have the potential to accelerate advancements in medical imaging research. Our code, pre-trained models, and generated data are available at <https://github.com/ibrahimethemhamamci/GenerateCT>.

1 Introduction

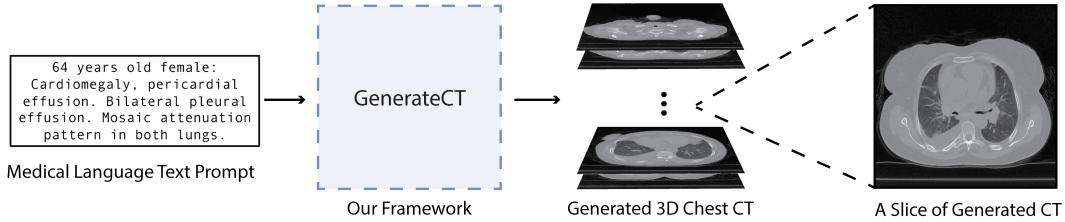


Figure 1: GenerateCT is a cascaded framework that generates high-fidelity 3D chest CT volumes with arbitrary slice numbers using medical language text prompts as conditioning inputs.

Generative modeling has experienced remarkable progress in recent years, especially in the domains of text-to-image [1, 2, 3, 4, 5, 6, 7, 8, 9, 10] and text-to-video [11, 12, 13, 14, 15, 16, 17, 18, 19, 20] synthesis. Despite these advancements, the medical field has not yet fully capitalized on the potential of large-scale foundational models [21]. Synthetic data generation, however, holds great promise for accelerating medical research, as medical imaging research faces significant challenges regarding data, such as patient privacy concerns, imbalanced class distribution, the requirement for trained clinicians, and the scarcity of extensive publicly available datasets [22].

*Correspondence: ibrahim.hamamci@uzh.ch.

Paired datasets of medical images and radiology reports offer immense potential for text-conditional medical image generation. This is because radiology reports provide a comprehensive assessment of a patient’s condition, thereby facilitating the efficient description of medical images. Consequently, the integration of chest radiographs and radiology reports has garnered significant interest in text-to-image generation [23]. This interest is due, in part, to the availability of multiple datasets [24, 25], and pre-trained open-source text-to-image models [3]. Despite these advancements, no previous study has explored the text-conditional generation of 3D medical images, such as Computed Tomography (CT) and Magnetic Resonance Imaging (MRI), using medical language text prompts. This gap in research is due to a lack of available paired radiology report-3D medical imaging data [26], the high computational demands of text-conditional video or 3D image generation models [27], and a limited amount of open-source work compared to 2D generation efforts [28].

In this paper, we address these limitations and present the first method for **text-conditional chest CT generation** (Fig. 1), making the entire framework fully open-source to accelerate 3D medical imaging research. Our method, **GenerateCT**, consists of a pre-trained T5X text encoder [29], a transformer-based text conditional 3D chest CT generation architecture, followed by a text-conditional spatial super-resolution diffusion model (Fig. 2). To the best of our knowledge, no publicly available dataset of 3D medical images with radiology reports exists for training our method [30]. Therefore, we also introduce a novel dataset of chest CT volumes with radiology reports to address this limitation.

Generating CT volumes, which are essentially 3D images composed of a series of 2D slices whose count determines the depth, presents a notable challenge: developing a compact model that can not only handle variable numbers of axial slices but also keep the token count to a minimum for computational efficiency. To address this, our work introduces the CT Vision Transformer (CT-ViT), a model inspired and further refined from previous work [31] and further tailored for 3D CT generation. CT-ViT deftly compresses CT volumes across all dimensions while maintaining auto-regressiveness in-depth, enabling the generation of CT volumes with a variable number of slices.

Upon obtaining a compressed representation of 3D CT volumes using CT-ViT, the text-to-CT task can be framed as a sequence-to-sequence problem to predict CT tokens based on the corresponding text embeddings. Drawing inspiration from prior work on image generation [32], our method employs a bidirectional transformer capable of predicting multiple CT tokens simultaneously. The transformer is trained using a proxy task closely related to mask prediction [33]. At inference, we initially designate all CT tokens as masked tokens. Subsequently, in each inference step, we make parallel predictions for all masked CT tokens, conditioning them on the text embeddings and unmasked (predicted) CT tokens. This approach is inspired by a previous study on video generation [18].

Building upon the ideas presented in previous work [4], we employ a text-conditional spatial super-resolution diffusion model following the generation of a low-resolution 3D chest CT with our transformer-based method, conditioned on medical language text prompts. The generated CT and the corresponding text prompt serve as conditioning inputs for the subsequent diffusion model. This strategy yields a spatially upsampled CT, inspired by the Cascaded Diffusion Model (CDM) [9].

As the first to explore text-conditional 3D medical image generation, GenerateCT lacks benchmarks for comparison. Thus, we validate our framework by applying the generated CT volumes to a potential real-world clinical application. We examine whether training on generated CT volumes yields similar performance to training on real CT volumes for multi-abnormality classification. Experiments and results demonstrate the ability of GenerateCT to produce realistic, high-fidelity 3D chest CT volumes consistent with free-form medical language text prompts. We make our code and trained models publicly available to facilitate the generation of chest CT volumes, encourage further research, and establish a baseline for future studies. Our contributions can be summarized as follows:

- We introduce GenerateCT, the first text-to-CT generation framework, and present the first results in the field of text-conditional 3D medical image generation.
- We propose CT-ViT, which enables the encoding and decoding of 3D CT volumes with variable numbers of axial slices. CT-ViT’s flexibility in handling varying sizes of 3D images in depth allows it to serve as a pre-trained model for different 3D medical domains.
- We demonstrate the potential of GenerateCT for clinical applications by training a model on generated chest CT volumes for multi-abnormality classification.
- We make our complete effort publicly available, including our code and trained models, with the aim of accelerating advancements in medical imaging research.

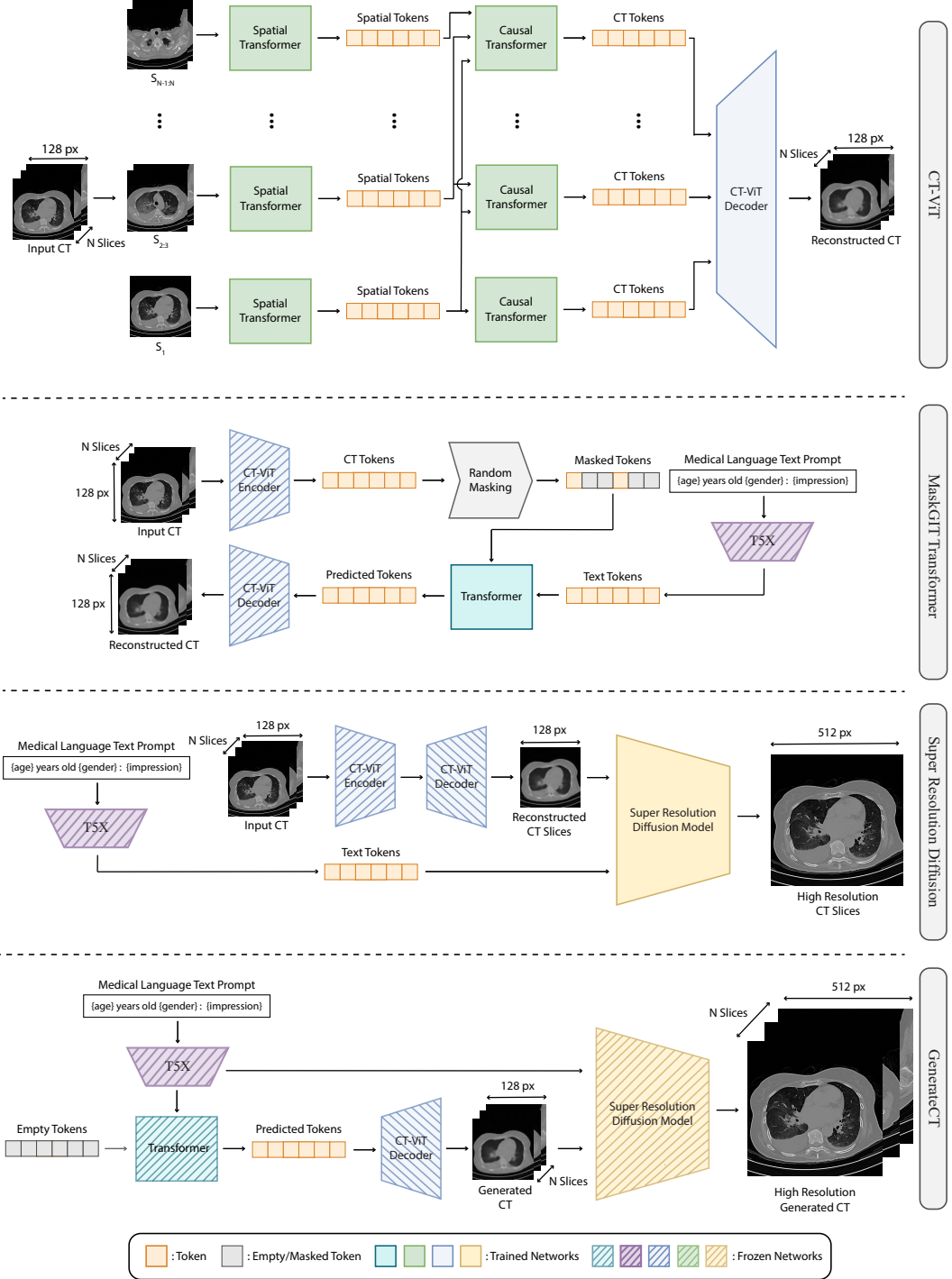


Figure 2: The GenerateCT architecture consists of three main components. (1) The CT-ViT encoder architecture processes the embeddings of CT patches from raw slices S through a spatial transformer followed by a causal transformer (auto-regressive in-depth), generating CT tokens. (2) The MaskGIT Transformer is trained to reconstruct masked tokens based on the frozen CT-ViT encoder’s predictions, conditioned on T5X text prompt tokens. (3) A text-conditional Diffusion model is employed to upsample CT slices. Finally, GenerateCT demonstrates the capability to generate high-resolution CT volumes with arbitrary slice numbers using medical language text prompts.

2 Related Works

Text-conditioned video generation. This field, split into two primary research streams: diffusion-based [19, 16, 34, 35, 20] and transformer-based auto-regressive methods [18, 13, 15, 12], has seen significant advancements. Diffusion-based techniques, utilizing 3D U-Net architectures, typically generate shorter, low-resolution videos with a preset number of frames, but can enhance resolution and duration through cascaded diffusion models [19]. In contrast, transformer-based methods offer adaptability, handling variable frame numbers and producing longer videos, albeit at lower dimensions [36]. In this context, our method extends the concept of text-conditional video generation to 3D medical imaging, essentially treating CT volumes as a sequence of 2D images. GenerateCT synergistically combines a transformer-based [18] and a diffusion-based method [19]. This innovative fusion enables the generation of high-resolution CT volumes with flexible and increased slice counts.

Text-conditioned medical image generation. Due to the increasing demand for high-fidelity medical data, medical image generation has emerged as an important research direction. Recent studies [23, 22] have explored the generation of 2D medical images based on medical language text prompts. These studies have successfully adapted pre-trained latent diffusion models [3], using publicly available chest X-rays and corresponding radiology reports [24]. However, there remains a clear gap in extending these models to the domain of 3D medical imaging, which introduces additional complexities and requires data richness. In this work, we introduce GenerateCT, a pioneering model capable of generating 3D chest CT scans from medical language text prompts. This novel approach has the potential to revolutionize the generation and utilization of medical imaging data, particularly in scenarios where real patient data is limited or challenging to acquire.

Datasets for text-conditioned medical image generation. Training models to generate medical images from text requires paired imaging data with corresponding radiology reports. While publicly available 2D imaging datasets like MIMIC-CXR [24] exist, there is a scarcity of publicly accessible 3D medical imaging datasets with radiology reports. Creating such datasets is challenging due to their larger size, the expertise required for annotating 3D images, and strict data sharing restrictions. The limited availability of such datasets is evident, as even a study focusing on multi-abnormality detection in chest CT volumes [37] made only a small portion of their dataset publicly accessible. This highlights the urgent need for more publicly available 3D medical imaging data and the potential for text-conditional 3D medical image data generation, which can drive further research in this field. To address this challenge, we collected a new dataset of chest CT volumes paired with radiology reports, which serves as a valuable resource for training our framework. Although the real dataset is not publicly available due to restrictions from the hospital, we are making our trained models public to enable researchers to generate their own data using text prompts. This open-access approach allows the wider research community to benefit from our work and advance 3D medical imaging research. Additionally, we are releasing the generated data used in Section 4.3 as examples from GenerateCT to provide tangible illustrations of text-conditional medical image generation.

3 Method

3.1 Dataset Preparation

Our dataset comprises 25,701 non-contrast 3D chest CT volumes with a resolution of 512×512 and varying axial slice counts ranging from 100 to 600. These volumes originate from 21,314 unique patients and have been reconstructed using multiple methods appropriate for different window settings [38]. This results in a total of 49,138 CT volumes, considering different reconstruction methods. We partitioned the volumes into a training set comprising 95% of the data and a testing set comprising 5%, ensuring no patient overlap between them. Each CT volume is accompanied by metadata that includes the patient's age, gender, and imaging specifics. Moreover, these volumes are paired with radiological reports that are categorized into separate sections: clinical information, technique, findings, and impression. The text prompts are formatted as "`{age} years old {gender}: {impression}`" using the impression section and metadata (Fig. 1). We convert the CT volumes into their respective Hounsfield Units (HU) using the slope and intercept values retrieved from the metadata. These values are clipped to the range $[-1000 \text{ HU}, +1000 \text{ HU}]$, representing the practical lower and upper limits of the HU scale [39, 40]. For training the text-conditioned CT generation

network, these values are normalized to $[-1, 1]$. However, for the diffusion model, these values are normalized to $[0, 1]$. The use of the dataset has been approved by the ethics committee.

3.2 GenerateCT: A Cascaded Architecture

GenerateCT (Fig. 2) is a three-component framework designed to generate high-resolution chest CT volumes guided by text. It comprises CT-ViT encoder-decoder (Section 3.2.1), MaskGIT Transformer (Section 3.2.2), and Diffusion-based model (Section 3.2.3) as described below.

$$\text{CT-ViT Training: } x^{\text{lowres}'} = f_{\text{dec}}(f_{\text{enc}}(x^{\text{lowres}})) \quad (\text{a})$$

$$\text{Transformer Training: } x_{\text{generated}}^{\text{lowres}} = f_{\text{dec}}(f_{\text{transformer}}(f_{\text{mask}}(f_{\text{enc}}(x^{\text{lowres}})), f_{\text{T5X}}(\text{txt}))) \quad (\text{b})$$

$$\text{Diffusion Training: } x_i^{\text{highres}} = f_{\text{diffusion}}(x_i^{\text{lowres}'}, f_{\text{T5X}}(\text{txt})) \quad (\text{c})$$

The CT-ViT encoder (Eq. a) transforms chest CT volumes into discrete representations called CT tokens. To achieve this, the encoder-decoder network, $f_{\text{dec}}(f_{\text{enc}})()$, is trained to predict $x^{\text{lowres}'}$, where $x^{\text{lowres}} \in \mathbb{R}^{(z_x+1) \times h_x \times w_x \times c_x}$ represents low-resolution chest CT volumes, where $z_x + 1$, h_x , w_x , and c_x denote the number of slices, height, width, and the number of channels of a given CT volume, respectively. The MaskGIT Transformer (Eq. b) works in conjunction with the CT-ViT encoder to convert text embeddings into corresponding CT tokens. These text embeddings are obtained using the pre-trained language model T5X [41], which has demonstrated efficacy in various natural language processing tasks, including medical text processing [42, 43]. The MaskGIT transformer model is trained to predict $x_{\text{generated}}^{\text{lowres}}$ from txt that denotes the medical language text prompt.

In consideration of the computational constraints inherent with high-resolution 3D images, the GenerateCT framework strategically first generates lower-dimensional CT volumes of dimensions $(128 \times 128 \times 201)$. The training process is further streamlined by maintaining a fixed number of frames, thereby reducing computational complexity. Subsequently, each slice undergoes enhancement via a text-conditioned 2D super-resolution diffusion model. This model (Eq. c), is designed to predict x_i^{highres} , the corresponding high-resolution chest CT slice, where i signifies the slice number.

$$\text{GenerateCT: } x_{\text{generated}}^{\text{highres}} = f_{\text{GenerateCT}}(e, f_{\text{T5X}}(\text{txt})) = f_{\text{diffusion}}(f_{\text{dec}}(f_{\text{transformer}}(e, f_{\text{T5X}}(\text{txt})))) \quad (\text{d})$$

At the inference stage, the GenerateCT framework, (Eq. d), generates high-resolution CT volumes guided by medical text prompts. Here, e represents the initial set of empty tokens, which forms the input for the transformer, which is conditioned on the text prompt processed by the T5X language model and generates a transformed low-resolution representation. This is then passed through the decoder function, and finally, the diffusion model enhances each slice to high-resolution. The flexibility of this framework allows the generation of high-resolution CT volumes with a variable number of slices, where the number of slices is determined by the number of empty tokens e .

3.2.1 CT-ViT Encoder

CT-ViT, illustrated in Fig. 2 and described in Eq. a, the first component of GenerateCT, is designed to provide a compact representation of CT volumes with a variable number of axial slices. CT-ViT is directly adapted from ViViT [31], a transformer model for video encoding that treats videos as a sequence of frames. We modify ViViT to perform causal attention to obtain an autoregressive encoder-decoder network allowing for a variable number of input slices, which are necessary to generate 3D medical images with different slice numbers inspired by C-ViViT [18]. This versatility proves advantageous when working with datasets with diverse frame numbers, typical of CT volumes. Moreover, this architecture supports pre-training with 2D images, further enhancing its utility.

The encoder processes a CT volume, denoted as $x \in \mathbb{R}^{(z_x+1) \times h_x \times w_x \times c_x}$, into CT tokens. The first set of tokens is solely tied to the initial CT slice, while the remaining tokens carry the volumetric information for the rest of the slices. The CT-ViT decoder reverses this process by transforming the tokens back into their original voxel space, resulting in a CT volume. It maintains the axial dimensionality of the input volume, supporting the generation of CT volumes with variable slice numbers. Patch division leads to smaller coronal and sagittal dimensions in the output volume compared to the input, translating into a lower-resolution yet more compact representation. To develop a discrete latent space, the model incorporates a vector quantization process. The training process also involves a combination of several loss functions, including L2 loss from ViT-VQGAN [44], image perceptual loss L_{IP} [45], video perceptual loss L_{VP} using the I3D network [46] as a feature extractor, and adversarial loss L_{Adv} with the StyleGAN [47], following the C-ViViT architecture.

3.2.2 MaskGIT Transformer

The second component of GenerateCT, the MaskGIT transformer, leverages CT tokens produced by CT-ViT and the embeddings of a text prompt to generate a 3D chest CT volume. This approach, inspired by a video generation model [18], combines Masked Visual Token Modeling [32] and classifier-free guidance [48, 5] during training, enhancing its adaptability to the provided data.

The MaskGIT transformer (refer to Fig. 2, Eq. b) randomly masks a certain percentage of CT tokens. It then reconstructs these masked CT tokens using the unmasked CT tokens and text prompt embeddings. These embeddings are obtained by passing the text prompt through the T5X encoder [29] and replicating the resulting text embeddings to align with the number of CT tokens.

The MaskGIT transformer integrates the masked CT tokens with text embeddings and processes them through a transformer decoder. This decoder mirrors the structure of transformer blocks in the CT-ViT’s encoder but with a critical distinction. Each block’s multi-head self-attention (MHSA) layer [49] in the decoder is tailored to permit each token to attend to all others, enriching the global context and bolstering the reconstruction of the masked CT tokens.

During inference, all CT tokens are initially assigned as masked tokens. The transformer decoder, at each step, concurrently predicts all masked CT tokens, conditioning them on the text embeddings and previously predicted CT tokens. After several iterations, all CT tokens are unmasked, resulting in a low-resolution 3D chest CT volume that is conditioned on a medical language text prompt.

3.2.3 Diffusion-Based Text-Conditional Super-Resolution

The final component of GenerateCT is a diffusion-based, text-conditional 2D super-resolution model, designed to increase the resolution of the initially produced low-resolution CT images (Fig. 2, Eq. c). This model, taking inspiration from prior work [4], favors a 2D diffusion process over a 3D one due to its more feasible computational needs and flexibility in handling 3D volumes with varying slice numbers. For text conditioning, the model employs the same medical language text prompt used during the 3D generation phase, applying it individually to each slice of the CT volume.

Our diffusion model, drawing from the Cascaded Diffusion Model [9], refines U-Net-based diffusion models [50, 51] with key alterations. The original self-attention layers are replaced with a single cross-attention layer at the final stage [52]. This architecture greatly enhances memory efficiency, facilitating the generation of high-resolution images that are conditioned on both a low-resolution slice and a medical language text prompt. Consequently, this diffusion model produces high-resolution CT volumes closely aligned with the provided text prompts and initial low-resolution slices.

4 Experiments

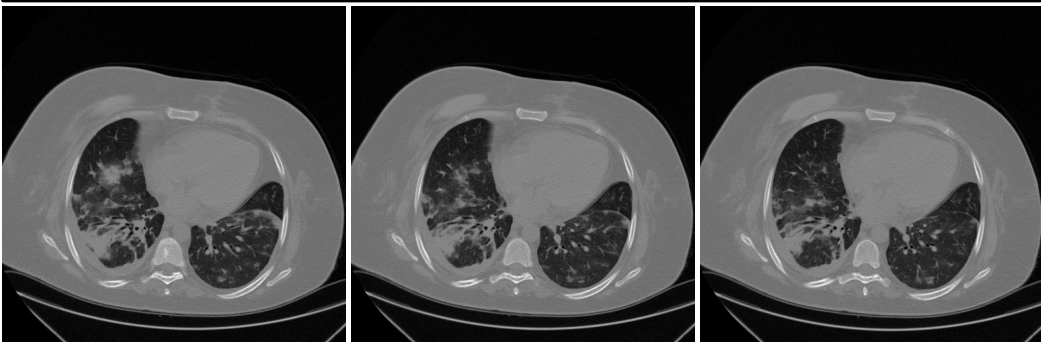
4.1 Implementation Details

We trained our CT-ViT encoder on our dataset, comprising 49,138 CT volumes, each resized to a resolution of $128 \times 128 \times 201$. We employed the Adam optimizer [53] with β_1 and β_2 hyperparameters set to 0.9 and 0.99, respectively, a learning rate of 0.00003, and an effective batch size of 32. The training was conducted for one week on a node with 8 A100 GPUs, completing 100,000 iterations. Subsequently, we trained the MaskGIT transformer using a paired dataset, which included the same CT volumes with the same resolution as CT-ViT and their corresponding medical language text prompts (Fig. 2). The Adam optimizer was used with identical β_1 and β_2 values, and the learning rate was maintained at 0.00003. However, we adjusted the effective batch size to 4 and introduced a cosine annealing warmup scheduler with a warmup phase of 10,000 steps and a maximum limit of 4,000,000 steps. This training stage, also executed on 8 A100 GPUs, lasted one week, concluding after 500,000 iterations. Finally, we trained the super-resolution model on a dataset of 9,876,738 CT slices, each initially resized to 128×128 by the encoder-decoder network. The super-resolution model then upsampled these to 512×512 , using the original volumes as ground truth. For this model, the same text prompts used for the 3D volumes were provided as conditioning for all slices of a CT. We retained the previous hyperparameters for the Adam optimizer and set the learning rate to 0.0005. This final training phase was carried out on 8 A100 GPUs over a week, reaching 175,000 iterations.

64 years old female: Cardiomegaly, pericardial effusion. Bilateral pleural effusion.



34 years old female: Bilateral consolidations and ground-glass opacities.



47 years old male: Bilateral mosaic attenuation pattern.



44 years old male: The overall examination is within normal limits.



Figure 3: Examples of text-conditional generation of Chest CT volumes within the practical HU scale limits of $[-1000 \text{ HU}, +1000 \text{ HU}]$. Each example includes three sequential slices from the same volume, highlighting GenerateCT's ability to maintain consistency across multiple slices.

4.2 Experimental Results

To evaluate the quality of the CT volumes generated by our model, we employed several metrics. We used the Fréchet Inception Distance (FID) [54] and the Fréchet Video Distance (FVD) [55], applying the latter over a span of 128×128 frames with the I3D model. For FVD evaluation, we resized the 3D volumes to $128 \times 128 \times 128$. Even though the diffusion model yields 2D slices, we assemble these slices into a CT volume to compute the FVD. To assess the effectiveness of our text-conditioned image generation, we additionally incorporated the CLIP score [56]. As a reference point, the original dataset, comprising paired CT images and corresponding medical text prompts, achieved a CLIP score of 27.4. The results of these metrics on our trained models are presented in Table 1. Given that our approach is the first of its kind for generating 3D CT volumes, there are currently no direct comparative benchmarks for evaluation. Hence, our method’s results primarily serve as a baseline for future research in this innovative area of text-conditioned 3D CT volume generation. This lack of comparative benchmarks underlines the novelty of the GenerateCT approach but also presents an exciting avenue for further research and development in this domain.

Table 1: Quantitative Results for GenerateCT and Its Components.

	Output Features			Metrics		
	Resolution	Dimension	Text-Guided	FID ↓	FVD ↓	CLIP ↑
CT-ViT	128	3D	No	73.4	1817.4	N/A
Transformer	128	3D	Yes	104.3	1886.8	25.2
Diffusion	512	2D	Yes	14.9	409.8	27.6
GenerateCT	512	3D	Yes	55.8	1092.3	27.1

In addition to our quantitative assessments, we also evaluate the performance of GenerateCT qualitatively. As seen in Fig. 3, each CT volume has been generated in response to a specific prompt, illustrating the GenerateCT’s ability to interpret and translate textual instructions into a corresponding chest CT volume. Notably, GenerateCT manages to maintain consistency across multiple slices of the same volume, demonstrating its aptitude for generating coherent and continuous 3D structures.

4.3 Evaluating GenerateCT via Training an Abnormality Classification Model

Given the absence of comparable benchmarks for our novel methodology, we explored its potential clinical applications by incorporating it into a larger radiological analysis framework. To cover this gap, we generated a novel dataset of CT volumes using GenerateCT to mirror the number and distribution of the Rad-ChestCT dataset [37], which consists of 3630 Chest CT volumes, each coupled with corresponding abnormality classification labels. We utilized this synthesized data to train a classification model [37]. The classification model was subjected to training on three distinct datasets: the original Rad-ChestCT dataset, the entirely synthesized dataset created by GenerateCT, and a composite dataset combining both real and generated images. In the evaluation, the model, when trained with our generated data, achieved a validation accuracy comparable to the accuracy obtained when using the original dataset. Significantly, the model demonstrated superior performance when trained on the composite dataset. This outcome indicates that our GenerateCT approach could serve as a valuable tool for data augmentation. For a more detailed breakdown of the training process and the specific accuracy achieved for each abnormality type, please see the supplementary document.

5 Limitations

While GenerateCT represents a pioneering effort, there are several limitations to consider:

Lack of established benchmarks. As the first method for text-conditional chest CT generation, GenerateCT currently lacks established benchmarks or comparative metrics to comprehensively evaluate its performance. Future research should incorporate additional methodologies and conduct ablation studies to facilitate meaningful comparisons with GenerateCT’s performance. While the current study demonstrates the potential of the proposed framework in multi-abnormality classification and exhibits promising qualitative results, further validation using diverse quantitative metrics is essential for a comprehensive assessment of the method’s capabilities.

2D super-resolution. Due to computational limitations, we employ a slice-by-slice super-resolution approach rather than a 3D volume super-resolution. Since we are using radiology reports for text conditioning, they may not accurately represent each individual slice. Consequently, a 3D super-resolution method could potentially yield better results but would restrict our framework’s ability to generate CT volumes with varying axial slice counts. Future research should explore the possibility of integrating 3D super-resolution while retaining flexibility for diverse axial slice counts.

Model generalization. Although CT-ViT is designed to accommodate varying 3D image sizes in-depth, its generalizability to other medical domains or imaging modalities (e.g., MRI) remains uncertain. Additionally, the framework’s applicability to non-chest CT volumes and other anatomical regions has yet to be investigated. Furthermore, the quantitative evaluation of GenerateCT’s performance in generating 3D CT volumes with varying numbers of axial slices has not been conducted.

Clinical relevance. Despite promising results in multi-abnormality classification, the quality and clinical relevance of the generated CT volumes require thorough evaluation. Potential issues such as artifacts, missing structures, or inconsistencies need to be addressed as they may impact their clinical utility. Additional research is needed to ensure the generated CT volumes meet the necessary quality standards and establish their relevance in various clinical applications.

Dataset limitations. Our novel dataset of chest CT volumes with radiology reports is a significant asset; limitations exist due to its size, diversity, and quality, which may affect the model’s generative performance. As it originates from a single institution, the dataset might suffer from representativeness issues, potential biases, and imbalanced class distribution, which could limit the model’s generalizability. To enhance the model’s generalizability, cross-institutional performance and robustness should be measured, and further training on multi-institutional data could improve its understanding of conditioning prompts and augment synthetic image diversity.

Impression section. Radiological reports are divided into sections such as clinical information, technique, findings, and impression. During training, we specifically utilize the impression sections corresponding to each volume. Although the impression sections provide valuable information, it’s important to acknowledge that they may not cover every aspect. Training the model on other sections, particularly findings, has the potential to enhance its conditioning capabilities.

Patient privacy concerns. Medical imaging research involving real patient data necessitates addressing patient privacy concerns. Synthetic data generation, such as our approach, has the potential to mitigate these concerns. However, despite anonymizing all textual data during the training process, potential risks of re-identifying individuals from generated volumes or their corresponding textual descriptions still warrant careful evaluation to ensure the privacy of patients is maintained.

Computational limitations. Despite its promising results, GenerateCT’s demand for high computational resources during training and inference phases could pose a challenge to its real-world application, particularly in environments where computational resources are scarce.

Future efforts should focus on overcoming limitations, improving volume quality and generalizability, and exploring additional medical applications to further validate the proposed framework’s utility.

6 Conclusion

In this paper, we present GenerateCT, the first method for text-conditional chest CT generation, addressing existing limitations in the field and making our entire framework fully open-source to promote further research in 3D medical imaging. We propose the CT-ViT for effectively compressing CT volumes while preserving auto-regressiveness in-depth, thereby enabling the generation of 3D CT volumes with varying numbers of axial slices. Our experiments validate the effectiveness of GenerateCT in generating realistic and high-fidelity 3D chest CT volumes that align with medical language text prompts. We further demonstrate the potential of our approach by training a model for multi-abnormality classification of chest CT volumes using the generated data. Our pioneering work represents the first step in text-conditional 3D medical image generation, providing valuable resources for the research community. We anticipate that GenerateCT will serve as a solid foundation for future advancements in this area and contribute to the development of innovative applications.

References

- [1] Ming Ding, Zhuoyi Yang, Wenyi Hong, Wendi Zheng, Chang Zhou, Da Yin, Junyang Lin, Xu Zou, Zhou Shao, Hongxia Yang, et al. Cogview: Mastering text-to-image generation via transformers. *Advances in Neural Information Processing Systems*, 34:19822–19835, 2021.
- [2] Aditya Ramesh, Prafulla Dhariwal, Alex Nichol, Casey Chu, and Mark Chen. Hierarchical text-conditional image generation with clip latents. *arXiv preprint arXiv:2204.06125*, 2022.
- [3] Robin Rombach, Andreas Blattmann, Dominik Lorenz, Patrick Esser, and Björn Ommer. High-resolution image synthesis with latent diffusion models. In *Proceedings of the IEEE/CVF Conference on Computer Vision and Pattern Recognition*, pages 10684–10695, 2022.
- [4] Chitwan Saharia, William Chan, Saurabh Saxena, Lala Li, Jay Whang, Emily L Denton, Kamyar Ghasemipour, Raphael Gontijo Lopes, Burcu Karagol Ayan, Tim Salimans, et al. Photorealistic text-to-image diffusion models with deep language understanding. *Advances in Neural Information Processing Systems*, 35:36479–36494, 2022.
- [5] Jiahui Yu, Yuanzhong Xu, Jing Yu Koh, Thang Luong, Gunjan Baid, Zirui Wang, Vijay Vasudevan, Alexander Ku, Yinfei Yang, Burcu Karagol Ayan, et al. Scaling autoregressive models for content-rich text-to-image generation. *arXiv preprint arXiv:2206.10789*, 2022.
- [6] Yogesh Balaji, Seungjun Nah, Xun Huang, Arash Vahdat, Jiaming Song, Karsten Kreis, Miika Aittala, Timo Aila, Samuli Laine, Bryan Catanzaro, et al. ediffi: Text-to-image diffusion models with an ensemble of expert denoisers. *arXiv preprint arXiv:2211.01324*, 2022.
- [7] Wenhui Chen, Hexiang Hu, Chitwan Saharia, and William W Cohen. Re-imagen: Retrieval-augmented text-to-image generator. *arXiv preprint arXiv:2209.14491*, 2022.
- [8] Shuyang Gu, Dong Chen, Jianmin Bao, Fang Wen, Bo Zhang, Dongdong Chen, Lu Yuan, and Baining Guo. Vector quantized diffusion model for text-to-image synthesis. In *Proceedings of the IEEE/CVF Conference on Computer Vision and Pattern Recognition*, pages 10696–10706, 2022.
- [9] Jonathan Ho, Chitwan Saharia, William Chan, David J Fleet, Mohammad Norouzi, and Tim Salimans. Cascaded diffusion models for high fidelity image generation. *J. Mach. Learn. Res.*, 23(47):1–33, 2022.
- [10] Alex Nichol, Prafulla Dhariwal, Aditya Ramesh, Pranav Shyam, Pamela Mishkin, Bob McGrew, Ilya Sutskever, and Mark Chen. Glide: Towards photorealistic image generation and editing with text-guided diffusion models. *arXiv preprint arXiv:2112.10741*, 2021.
- [11] Uriel Singer, Adam Polyak, Thomas Hayes, Xi Yin, Jie An, Songyang Zhang, Qiyuan Hu, Harry Yang, Oron Ashual, Oran Gafni, et al. Make-a-video: Text-to-video generation without text-video data. *arXiv preprint arXiv:2209.14792*, 2022.
- [12] Chenfei Wu, Lun Huang, Qianxi Zhang, Binyang Li, Lei Ji, Fan Yang, Guillermo Sapiro, and Nan Duan. Godiva: Generating open-domain videos from natural descriptions. *arXiv preprint arXiv:2104.14806*, 2021.
- [13] Chenfei Wu, Jian Liang, Lei Ji, Fan Yang, Yuejian Fang, Dixin Jiang, and Nan Duan. Nüwa: Visual synthesis pre-training for neural visual world creation. In *Computer Vision–ECCV 2022: 17th European Conference, Tel Aviv, Israel, October 23–27, 2022, Proceedings, Part XVI*, pages 720–736. Springer, 2022.
- [14] Daquan Zhou, Weimin Wang, Hanshu Yan, Weiwei Lv, Yizhe Zhu, and Jiashi Feng. Magicvideo: Efficient video generation with latent diffusion models. *arXiv preprint arXiv:2211.11018*, 2022.
- [15] Wenyi Hong, Ming Ding, Wendi Zheng, Xinghan Liu, and Jie Tang. Cogvideo: Large-scale pretraining for text-to-video generation via transformers. *arXiv preprint arXiv:2205.15868*, 2022.
- [16] Andreas Blattmann, Robin Rombach, Huan Ling, Tim Dockhorn, Seung Wook Kim, Sanja Fidler, and Karsten Kreis. Align your latents: High-resolution video synthesis with latent diffusion models. *arXiv preprint arXiv:2304.08818*, 2023.
- [17] Yogesh Balaji, Martin Renqiang Min, Bing Bai, Rama Chellappa, and Hans Peter Graf. Conditional gan with discriminative filter generation for text-to-video synthesis. In *IJCAI*, volume 1, page 2, 2019.

[18] Ruben Villegas, Mohammad Babaeizadeh, Pieter-Jan Kindermans, Hernan Moraldo, Han Zhang, Mohammad Taghi Saffar, Santiago Castro, Julius Kunze, and Dumitru Erhan. Phenaki: Variable length video generation from open domain textual description. *arXiv preprint arXiv:2210.02399*, 2022.

[19] Jonathan Ho, William Chan, Chitwan Saharia, Jay Whang, Ruiqi Gao, Alexey Gritsenko, Diederik P Kingma, Ben Poole, Mohammad Norouzi, David J Fleet, et al. Imagen video: High definition video generation with diffusion models. *arXiv preprint arXiv:2210.02303*, 2022.

[20] Jonathan Ho, Tim Salimans, Alexey Gritsenko, William Chan, Mohammad Norouzi, and David J Fleet. Video diffusion models. *arXiv preprint arXiv:2204.03458*, 2022.

[21] Aghiles Kebaili, Jérôme Lapuyade-Lahorgue, and Su Ruan. Deep learning approaches for data augmentation in medical imaging: A review. *Journal of Imaging*, 9(4):81, 2023.

[22] Hyungyung Lee, Wonjae Kim, Jin-Hwa Kim, Tackeun Kim, Jihang Kim, Leonard Sunwoo, and Edward Choi. Unified chest x-ray and radiology report generation model with multi-view chest x-rays. *arXiv preprint arXiv:2302.12172*, 2023.

[23] Pierre Chambon, Christian Blauthgen, Jean-Benoit Delbrouck, Rogier Van der Sluijs, Małgorzata Połacin, Juan Manuel Zambrano Chaves, Tanishq Mathew Abraham, Shivanshu Purohit, Curtis P Langlotz, and Akshay Chaudhari. Roentgen: Vision-language foundation model for chest x-ray generation. *arXiv preprint arXiv:2211.12737*, 2022.

[24] Alistair EW Johnson, Tom J Pollard, Seth J Berkowitz, Nathaniel R Greenbaum, Matthew P Lungren, Chih-ying Deng, Roger G Mark, and Steven Horng. Mimic-cxr, a de-identified publicly available database of chest radiographs with free-text reports. *Scientific data*, 6(1):317, 2019.

[25] Jeremy Irvin, Pranav Rajpurkar, Michael Ko, Yifan Yu, Silviana Ciurea-Ilcus, Chris Chute, Henrik Marklund, Behzad Haghighoo, Robyn Ball, Katie Shpanskaya, et al. Chexpert: A large chest radiograph dataset with uncertainty labels and expert comparison. In *Proceedings of the AAAI conference on artificial intelligence*, volume 33, pages 590–597, 2019.

[26] Nathaniel Linna and Charles E Kahn Jr. Applications of natural language processing in radiology: A systematic review. *International Journal of Medical Informatics*, page 104779, 2022.

[27] Aidan Clark, Jeff Donahue, and Karen Simonyan. Adversarial video generation on complex datasets. *arXiv preprint arXiv:1907.06571*, 2019.

[28] Chenshuang Zhang, Chaoning Zhang, Mengchun Zhang, and In So Kweon. Text-to-image diffusion model in generative ai: A survey. *arXiv preprint arXiv:2303.07909*, 2023.

[29] Colin Raffel, Noam Shazeer, Adam Roberts, Katherine Lee, Sharan Narang, Michael Matena, Yanqi Zhou, Wei Li, and Peter J Liu. Exploring the limits of transfer learning with a unified text-to-text transformer. *The Journal of Machine Learning Research*, 21(1):5485–5551, 2020.

[30] Youssef Skandarani, Pierre-Marc Jodoin, and Alain Lalande. Gans for medical image synthesis: An empirical study. *Journal of Imaging*, 9(3):69, 2023.

[31] Anurag Arnab, Mostafa Dehghani, Georg Heigold, Chen Sun, Mario Lučić, and Cordelia Schmid. Vivit: A video vision transformer. In *Proceedings of the IEEE/CVF international conference on computer vision*, pages 6836–6846, 2021.

[32] Huiwen Chang, Han Zhang, Lu Jiang, Ce Liu, and William T Freeman. Maskgit: Masked generative image transformer. In *Proceedings of the IEEE/CVF Conference on Computer Vision and Pattern Recognition*, pages 11315–11325, 2022.

[33] Jacob Devlin, Ming-Wei Chang, Kenton Lee, and Kristina Toutanova. Bert: Pre-training of deep bidirectional transformers for language understanding. *arXiv preprint arXiv:1810.04805*, 2018.

[34] Ruihan Yang, Prakhar Srivastava, and Stephan Mandt. Diffusion probabilistic modeling for video generation. *arXiv preprint arXiv:2203.09481*, 2022.

[35] Vikram Voleti, Alexia Jolicoeur-Martineau, and Christopher Pal. Masked conditional video diffusion for prediction, generation, and interpolation. *arXiv preprint arXiv:2205.09853*, 2022.

[36] Wilson Yan, Yunzhi Zhang, Pieter Abbeel, and Aravind Srinivas. Videogpt: Video generation using vq-vae and transformers. *arXiv preprint arXiv:2104.10157*, 2021.

[37] Rachel Lea Draelos, David Dov, Maciej A Mazurowski, Joseph Y Lo, Ricardo Henao, Geoffrey D Rubin, and Lawrence Carin. Machine-learning-based multiple abnormality prediction with large-scale chest computed tomography volumes. *Medical image analysis*, 67:101857, 2021.

[38] Martin J Willemink and Peter B Noël. The evolution of image reconstruction for ct—from filtered back projection to artificial intelligence. *European radiology*, 29:2185–2195, 2019.

[39] Tami D DenOtter and Johanna Schubert. Hounsfield unit, 2019.

[40] Ramit Lamba, John P McGahan, Michael T Corwin, Chin-Shang Li, Tien Tran, J Anthony Seibert, and John M Boone. Ct hounsfield numbers of soft tissues on unenhanced abdominal ct scans: variability between two different manufacturers’ mdct scanners. *AJR. American journal of roentgenology*, 203(5):1013, 2014.

[41] Adam Roberts, Hyung Won Chung, Anselm Levskaya, Gaurav Mishra, James Bradbury, Daniel Andor, Sharan Narang, Brian Lester, Colin Gaffney, Afroz Mohiuddin, et al. Scaling up models and data with t5x and seqio. *arXiv preprint arXiv:2203.17189*, 13, 2022.

[42] Rodrigo Nogueira, Zhiying Jiang, and Jimmy Lin. Document ranking with a pretrained sequence-to-sequence model. *arXiv preprint arXiv:2003.06713*, 2020.

[43] Long N Phan, James T Anibal, Hieu Tran, Shaurya Chanana, Erol Bahadroglu, Alec Peltekian, and Grégoire Altan-Bonnet. Scifive: a text-to-text transformer model for biomedical literature. *arXiv preprint arXiv:2106.03598*, 2021.

[44] Jiahui Yu, Xin Li, Jing Yu Koh, Han Zhang, Ruoming Pang, James Qin, Alexander Ku, Yuanzhong Xu, Jason Baldridge, and Yonghui Wu. Vector-quantized image modeling with improved vqgan. *arXiv preprint arXiv:2110.04627*, 2021.

[45] Justin Johnson, Alexandre Alahi, and Li Fei-Fei. Perceptual losses for real-time style transfer and super-resolution. In *Computer Vision–ECCV 2016: 14th European Conference, Amsterdam, The Netherlands, October 11–14, 2016, Proceedings, Part II 14*, pages 694–711. Springer, 2016.

[46] Joao Carreira and Andrew Zisserman. Quo vadis, action recognition? a new model and the kinetics dataset. In *proceedings of the IEEE Conference on Computer Vision and Pattern Recognition*, pages 6299–6308, 2017.

[47] Tero Karras, Samuli Laine, Miika Aittala, Janne Hellsten, Jaakko Lehtinen, and Timo Aila. Analyzing and improving the image quality of stylegan. In *Proceedings of the IEEE/CVF conference on computer vision and pattern recognition*, pages 8110–8119, 2020.

[48] Jonathan Ho and Tim Salimans. Classifier-free diffusion guidance. *arXiv preprint arXiv:2207.12598*, 2022.

[49] Ashish Vaswani, Noam Shazeer, Niki Parmar, Jakob Uszkoreit, Llion Jones, Aidan N Gomez, Łukasz Kaiser, and Illia Polosukhin. Attention is all you need. *Advances in neural information processing systems*, 30, 2017.

[50] Alexander Quinn Nichol and Prafulla Dhariwal. Improved denoising diffusion probabilistic models. In *International Conference on Machine Learning*, pages 8162–8171. PMLR, 2021.

[51] Chitwan Saharia, William Chan, Huiwen Chang, Chris Lee, Jonathan Ho, Tim Salimans, David Fleet, and Mohammad Norouzi. Palette: Image-to-image diffusion models. In *ACM SIGGRAPH 2022 Conference Proceedings*, pages 1–10, 2022.

[52] Iz Beltagy, Matthew E Peters, and Arman Cohan. Longformer: The long-document transformer. *arXiv preprint arXiv:2004.05150*, 2020.

[53] Diederik P Kingma and Jimmy Ba. Adam: A method for stochastic optimization. *arXiv preprint arXiv:1412.6980*, 2014.

[54] Martin Heusel, Hubert Ramsauer, Thomas Unterthiner, Bernhard Nessler, and Sepp Hochreiter. Gans trained by a two time-scale update rule converge to a local nash equilibrium. *Advances in neural information processing systems*, 30, 2017.

[55] Thomas Unterthiner, Sjoerd van Steenkiste, Karol Kurach, Raphaël Marinier, Marcin Michalski, and Sylvain Gelly. Fvd: A new metric for video generation, 2019.

[56] Jack Hessel, Ari Holtzman, Maxwell Forbes, Ronan Le Bras, and Yejin Choi. Clipscore: A reference-free evaluation metric for image captioning. *arXiv preprint arXiv:2104.08718*, 2021.

Supplementary Document for GenerateCT: Text-Guided 3D Chest CT Generation

This supplementary document extends the discussion and results presented in the main paper. It offers a more in-depth exploration of GenerateCT’s capabilities and potential in the field of text-conditional 3D medical image generation by providing more qualitative results and a detailed exploration of a practical clinical application of GenerateCT. Beyond the technical aspects, we provide insights into the broader impact of our research, along with information about the licensing terms. All our resources, including the code, pre-trained models, and generated data, can be accessed publicly via <https://github.com/ibrahimethemhamamci/GenerateCT>.

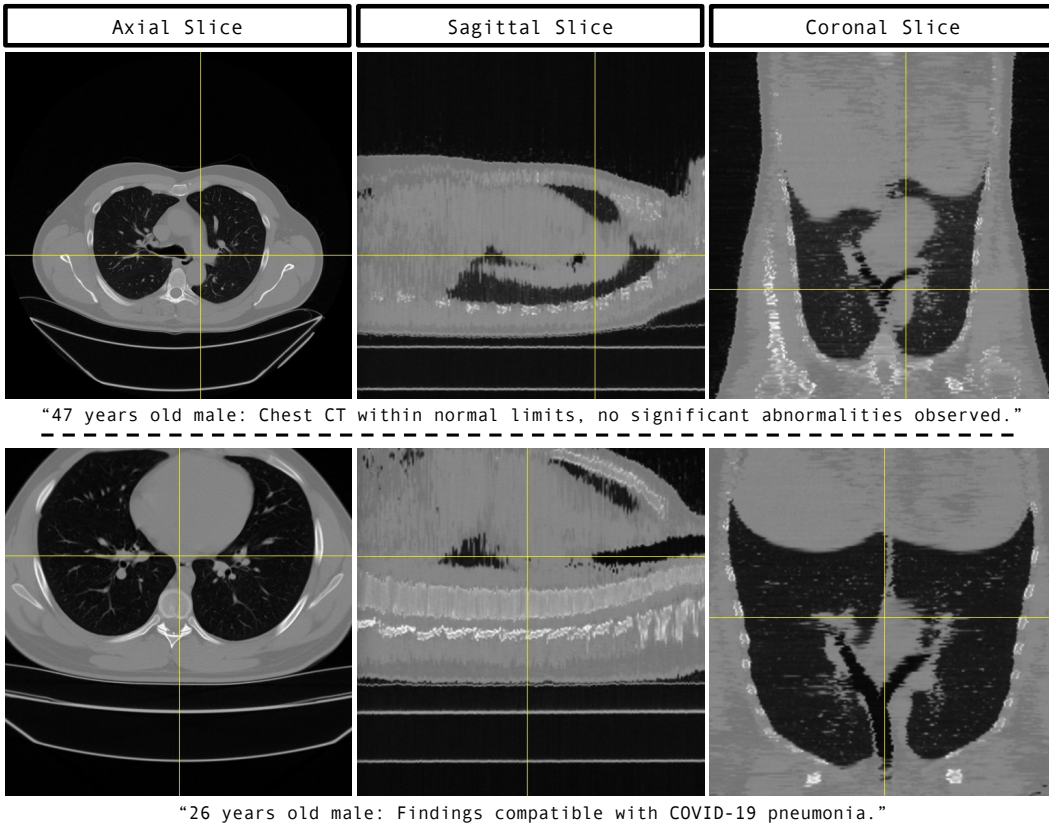


Figure 1: Sample slices from the axial, sagittal, and coronal planes of synthetic chest CT volumes, generated by GenerateCT in response to given medical language text prompts.

1 Qualitative Results

This section showcases the broad spectrum of results generated by GenerateCT. In Fig. 1, we display not only the axial slices of the generated 3D CT volumes but also the sagittal and coronal slices. These examples underscore GenerateCT’s proficiency in creating comprehensive 3D chest CT volumes based on specific medical language text prompts. Furthermore, in Fig. 2, we illustrate the outputs derived from the two components of GenerateCT. A corresponding slice from the original CT is also presented for comparison, demonstrating the realism achievable in the reconstructed and subsequently upsampled CT volumes. This underlines the efficacy and robustness of the training process.

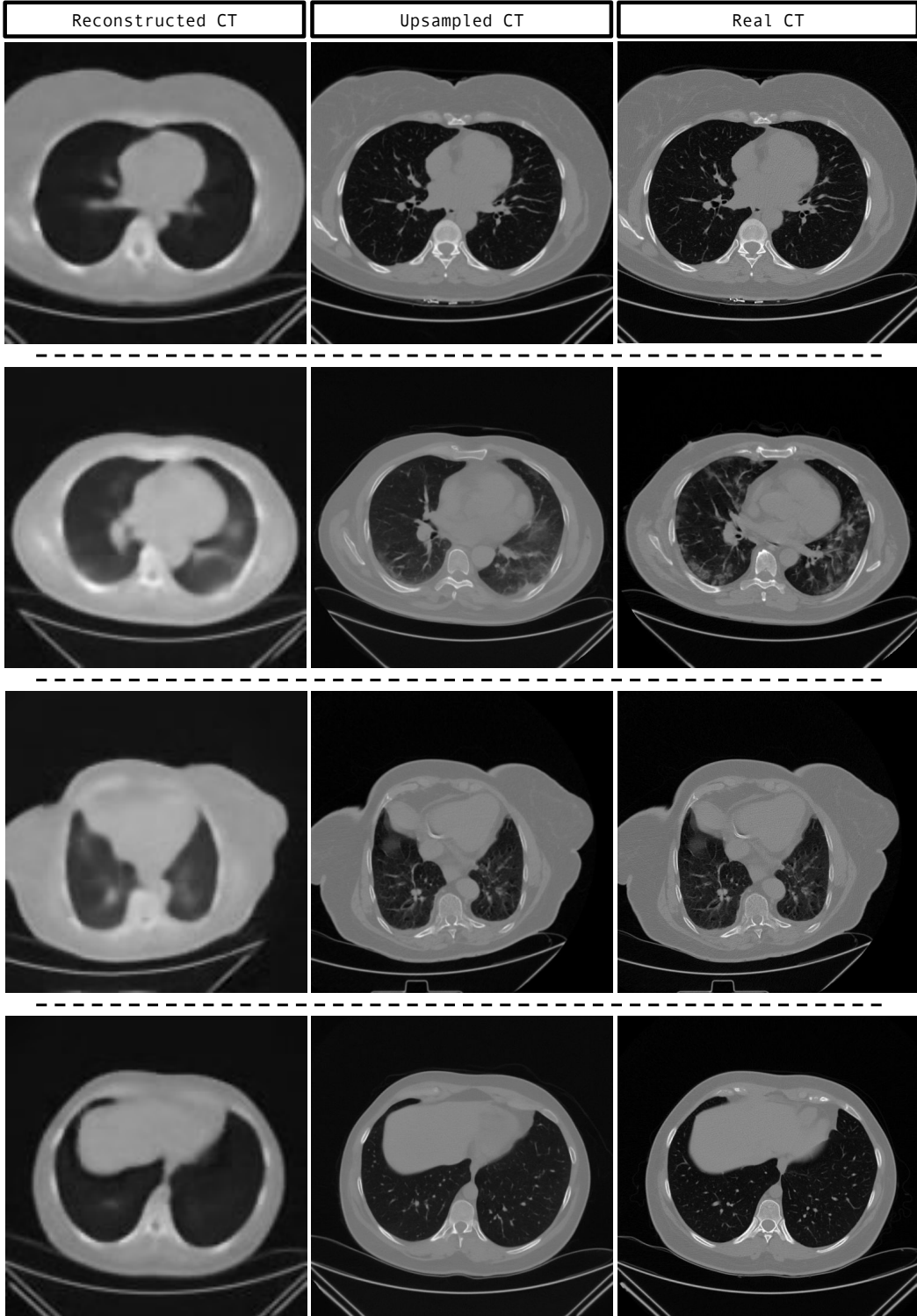


Figure 2: The two components of the GenerateCT architecture are visualized with sample outputs. The first component includes two sub-models: the CT-ViT, an encoder-decoder model that reconstructs low-resolution chest CT (Reconstructed CT), and the MaskGIT Transformer, which is not included in this figure. The second component, a diffusion model, enhances these CT slices to high-resolution (Upsampled CT) using both the text prompt and the low-resolution output from the first component. A slice from the original CT (Real CT) is also presented for comparison.

2 Evaluating GenerateCT via Training an Abnormality Classification Model

In this section, we take a closer look at a practical clinical application of GenerateCT. Through a case study, we illustrate how a multi-abnormality classification model can be trained using synthetic chest CT volumes generated by our approach based on medical language text prompts. This detailed examination highlights the significant potential of GenerateCT to enhance the medical imaging field, especially when acquiring real patient data is constrained or challenging.

2.1 Experimental Setup

Our experiments involved three distinctive training scenarios: (1) utilizing only the real patient data, (2) utilizing only the generated data by GenerateCT, and (3) implementing a hybrid approach by initially training with our generated data and later fine-tuning with the real patient data. Regardless of the scenario, all models were subjected to validation on the same real patient dataset.

The real patient data was derived from a publicly available dataset from a prior study [1] that concentrated on multi-abnormality detection in chest CT volumes. This dataset contains 2,286 CT volumes for training and 1,344 CT volumes for validation, each linked with corresponding abnormality labels for 83 unique abnormalities.

We constructed a synthetic training dataset via GenerateCT, replicating the volume count and abnormality distribution seen in the training set of real patient data. This led to the creation of an equal number of 2,286 synthetic CT volumes for training. The generation process is conducted by a pre-defined structure for medical language text prompts, "`{age} years old {gender}:{impression}`". Here, `{impression}` reflected the abnormality labels from the real training data. Given their non-availability in the real patient data, age, and gender parameters were assigned randomly.

To maintain experimental consistency, all CT volumes were resized to a resolution of $420 \times 420 \times 201$. Moreover, Hounsfield Units (HU) values of each volume were calibrated to a range of $[-1000, +200]$ as the main focus of the classification task was on heart and lung abnormalities [2].

Our study employed the CT-Net83 model [1], with its default parameters for the classification of 83 distinct radiological abnormalities. We used the Stochastic Gradient Descent optimizer [3] with a learning rate of 0.001 and a weight decay of 0.0000001. Each training session, conducted over 15 epochs with a batch size of 12 on three A6000 48G GPUs, took approximately 12 hours.

2.2 Experimental Results

We performed validation on the same real patient dataset for all three training scenarios. Table 1 documents the model's performance across each training scenario, exhibiting the area under the receiver operating characteristic (AUROC) and Average Precision (AP) for all 83 abnormalities.

A key observation from our findings is the comparable performance of the model trained on generated data and the model trained on real patient data, evidenced by the nearly equivalent evaluation scores from the real data set: with a mean AP of 0.177 and mean AUROC of 0.613 for real data, versus 0.146 and 0.536 respectively, for synthetic data. This observation is particularly compelling, given that both scenarios utilized the same real patient dataset for validation. Moreover, this dataset originated from a different institutional setup than the one used for GenerateCT training. In addition, the volume of synthetic training data was kept on par with real patient training data, despite the potential to generate an unlimited amount of synthetic data using GenerateCT. In addition, our findings reveal that initiating the training process with synthetic data before transitioning to real patient data resulted in enhanced model performance, evidenced by a modest increase in both mean AUROC (0.623) and mean AP (0.190). This underscores the potential of synthetic data as a resource for model training.

Given the results in Table 1, GenerateCT clearly stands as a valuable tool for data augmentation. Moreover, our experimental results underscore GenerateCT's ability to create detailed and realistic 3D chest CT volumes that accurately correspond to diverse text prompts.

These results represent a significant contribution to the field of medical imaging, suggesting that GenerateCT may be a potent tool for driving advancements in diagnosis and treatment planning. Furthermore, GenerateCT's potential to simulate realistic, high-resolution medical images based on textual descriptions presents a promising avenue for future research and applications in healthcare.

Table 1: Performance metrics (AUROC and Average Precision) for different abnormalities using different training datasets.

	Real Data		Generated Data		Composite Data		Test Set Ratio
	AUROC	AP	AUROC	AP	AUROC	AP	
Air trapping	0.561	0.044	0.621	0.050	0.633	0.051	0.033
Airspace disease	0.605	0.258	0.571	0.210	0.607	0.233	0.134
Aneurysm	0.577	0.015	0.493	0.012	0.587	0.020	0.014
Arthritis	0.515	0.284	0.510	0.298	0.505	0.282	0.285
Aspiration	0.616	0.091	0.518	0.051	0.624	0.092	0.066
Atelectasis	0.575	0.349	0.579	0.356	0.596	0.408	0.283
Atherosclerosis	0.550	0.314	0.473	0.281	0.525	0.297	0.284
Bandlike or linear	0.461	0.156	0.511	0.191	0.483	0.166	0.155
Breast implant	0.387	0.016	0.325	0.012	0.550	0.066	0.012
Breast surgery	0.499	0.030	0.504	0.026	0.484	0.037	0.018
Bronchial wall thickening	0.556	0.080	0.474	0.074	0.566	0.086	0.085
Bronchiectasis	0.704	0.313	0.543	0.179	0.666	0.234	0.14
Bronchiolectasis	0.739	0.068	0.475	0.021	0.683	0.044	0.016
Bronchiolitis	0.443	0.024	0.492	0.025	0.509	0.026	0.018
Bronchitis	0.533	0.010	0.567	0.023	0.570	0.011	0.007
CABG	0.754	0.118	0.504	0.068	0.764	0.115	0.04
Calcification	0.426	0.669	0.501	0.727	0.428	0.676	0.67
Cancer	0.593	0.614	0.523	0.575	0.618	0.636	0.28
Cardiomegaly	0.752	0.238	0.622	0.142	0.798	0.314	0.09
Catheter or port	0.660	0.218	0.591	0.120	0.681	0.266	0.105
Cavitation	0.604	0.056	0.493	0.058	0.589	0.056	0.035
Chest tube	0.864	0.123	0.640	0.037	0.881	0.173	0.02
Clip	0.488	0.098	0.532	0.117	0.491	0.106	0.084
Congestion	0.885	0.042	0.701	0.015	0.951	0.266	0.002
Consolidation	0.690	0.286	0.565	0.193	0.680	0.256	0.151
Coronary artery disease	0.567	0.608	0.500	0.568	0.582	0.607	0.494
Cyst	0.497	0.169	0.469	0.156	0.488	0.162	0.143
Debris	0.697	0.081	0.572	0.048	0.697	0.111	0.031
Deformity	0.580	0.062	0.475	0.051	0.551	0.057	0.062
Density	0.536	0.106	0.499	0.095	0.538	0.116	0.09
Dilation or ectasia	0.571	0.063	0.458	0.051	0.589	0.066	0.051
Distention	0.592	0.020	0.653	0.056	0.641	0.019	0.012
Emphysema	0.623	0.329	0.421	0.230	0.614	0.352	0.243
Fibrosis	0.792	0.332	0.574	0.152	0.775	0.259	0.112
Fracture	0.601	0.094	0.536	0.075	0.588	0.097	0.065
GI tube	0.900	0.192	0.710	0.067	0.910	0.269	0.022
Granuloma	0.448	0.071	0.411	0.066	0.450	0.071	0.083
Groundglass	0.594	0.415	0.524	0.341	0.589	0.422	0.332
Hardware	0.447	0.022	0.513	0.028	0.416	0.021	0.017
Heart failure	0.878	0.056	0.585	0.013	0.951	0.199	0.002
Heart valve replacement	0.745	0.043	0.721	0.059	0.858	0.165	0.018
Hemothorax	0.889	0.125	0.721	0.011	0.833	0.032	0.004
Hernia	0.523	0.120	0.488	0.126	0.548	0.126	0.12
Honeycombing	0.903	0.258	0.566	0.045	0.846	0.105	0.027
Infection	0.539	0.355	0.448	0.301	0.538	0.354	0.333
Infiltrate	0.413	0.015	0.438	0.021	0.352	0.014	0.015
Inflammation	0.529	0.087	0.429	0.076	0.521	0.086	0.082
Interstitial lung disease	0.739	0.362	0.565	0.196	0.742	0.304	0.153
Lesion	0.467	0.234	0.487	0.246	0.482	0.235	0.238
Lucency	0.574	0.028	0.567	0.028	0.556	0.041	0.018
Lung resection	0.519	0.222	0.516	0.236	0.545	0.242	0.194
Lymphadenopathy	0.682	0.260	0.580	0.191	0.686	0.272	0.167
Mass	0.498	0.123	0.541	0.149	0.505	0.128	0.12
Mucous plugging	0.519	0.028	0.413	0.027	0.480	0.027	0.037
Nodule	0.649	0.858	0.600	0.855	0.682	0.873	0.779
Nodule >1cm	0.515	0.136	0.544	0.158	0.499	0.121	0.118
Opacity	0.369	0.456	0.539	0.571	0.634	0.667	0.538

Table 1 – continued from previous page

	Real Data		Generated Data		Composite Data		Test Set Ratio
	AUROC	AP	AUROC	AP	AUROC	AP	
Pacemaker/defibrillator	0.778	0.128	0.563	0.079	0.857	0.261	0.039
Pericardial effusion	0.626	0.207	0.544	0.167	0.629	0.236	0.15
Pericardial thickening	0.501	0.024	0.551	0.076	0.538	0.026	0.035
Plaque	0.608	0.034	0.408	0.023	0.566	0.031	0.017
Pleural effusion	0.770	0.424	0.656	0.308	0.792	0.507	0.195
Pleural thickening	0.583	0.120	0.573	0.125	0.549	0.118	0.086
Pneumonia	0.629	0.079	0.569	0.067	0.664	0.096	0.039
Pneumonitis	0.677	0.070	0.578	0.034	0.689	0.052	0.026
Pneumothorax	0.780	0.196	0.576	0.030	0.815	0.193	0.028
Postsurgical	0.554	0.525	0.517	0.503	0.537	0.521	0.428
Pulmonary edema	0.816	0.144	0.638	0.081	0.852	0.217	0.052
Reticulation	0.747	0.211	0.559	0.121	0.710	0.165	0.094
Scarring	0.448	0.193	0.462	0.219	0.531	0.247	0.205
Scattered calcifications	0.519	0.187	0.506	0.190	0.491	0.187	0.168
Scattered nodules	0.497	0.216	0.463	0.211	0.494	0.225	0.21
Secretion	0.587	0.019	0.530	0.019	0.599	0.021	0.015
Septal thickening	0.793	0.176	0.612	0.105	0.794	0.195	0.071
Soft tissue	0.475	0.166	0.558	0.206	0.466	0.160	0.138
Staple	0.501	0.032	0.536	0.040	0.462	0.033	0.02
Stent	0.580	0.040	0.550	0.064	0.554	0.037	0.037
Sternotomy	0.743	0.186	0.536	0.086	0.779	0.241	0.071
Suture	0.507	0.028	0.534	0.022	0.466	0.022	0.023
Tracheal tube	0.937	0.234	0.710	0.033	0.931	0.232	0.017
Transplant	0.701	0.174	0.574	0.099	0.713	0.178	0.057
Tree in bud	0.573	0.064	0.399	0.020	0.591	0.035	0.03
Tuberculosis	0.534	0.005	0.366	0.003	0.467	0.006	0.014

3 Broader Impacts

Our study introduces GenerateCT, a pioneering effort towards the text-conditional generation of 3D medical imaging, specifically chest CT volumes. By bridging the gap in current research, we anticipate positive impacts on medical research and healthcare, particularly in scenarios where real patient data is limited or challenging to procure. Nonetheless, the ethical and societal implications of our work are essential to consider.

The primary ethical concern is the potential misuse of our method. The ability to generate high-fidelity, realistic CT volumes from text prompts could potentially be used to create synthetic medical data misrepresented as real. This could result in incorrect diagnoses, insurance fraud, or even unwarranted anxiety among patients, with profound implications on healthcare systems and public trust. Another concern relates to data privacy. The pairing of medical images with radiology reports necessitates a careful and stringent data privacy strategy to protect the identities and sensitive health information of the individuals included in the training data. The technology also poses challenges related to fairness. It relies heavily on data availability and quality; thus, biases in the input data, such as the underrepresentation of certain demographic groups or medical conditions, could lead to biases in the generated images. These biases could reinforce existing health inequities.

Despite these challenges, there are potential mitigation strategies. To discourage misuse, robust watermarking techniques could be developed to differentiate real and generated images. In forthcoming research, data privacy concerns can be rigorously addressed by adopting and enforcing anonymization and data protection protocols, as we diligently implemented in this study. For fairness considerations, we encourage efforts towards broad and diverse data collection and developing strategies to identify and correct potential biases in the training data.

While this work focuses on generating chest CT volumes from medical language text prompts, it opens the door for generating other types of 3D medical images. Although such expansion of this technology could benefit medical research, each specific application may bring its unique potential risks and ethical considerations, which should also be carefully evaluated.

Finally, our decision to make our code and models publicly available is driven by a commitment to open science and the advancement of medical imaging research. However, we understand that open access can also pose risks, and we encourage the research community to use our models responsibly, considering potential negative societal impacts. This includes being mindful of the limitations and potential misuse of synthetic data and not using it as a direct substitute for real patient data in clinical settings without thorough validation and ethical review.

In conclusion, GenerateCT has the potential to catalyze medical imaging research, improve healthcare outcomes, and drive innovations in synthetic data generation. Still, it is crucial to actively tackle potential negative societal impacts. We are dedicated to keeping up discussions and partnerships to help navigate these complex ethical issues. Our goal is to balance tech advancement with society's well-being and ethical responsibility.

4 License

Our work, including the codes, models, and generated data, is released under a Creative Commons Attribution (CC-BY) license¹. This means that anyone is free to share (copy and redistribute the material in any medium or format) and adapt (remix, transform, and build upon the material) for any purpose, even commercially, as long as appropriate credit is given, a link to the license is provided, and any changes that were made are indicated. This aligns with our goal of facilitating progress in the field by providing a resource for researchers to build upon.

References

- [1] Rachel Lea Draelos, David Dov, Maciej A Mazurowski, Joseph Y Lo, Ricardo Henao, Geoffrey D Rubin, and Lawrence Carin. Machine-learning-based multiple abnormality prediction with large-scale chest computed tomography volumes. *Medical image analysis*, 67:101857, 2021.
- [2] Tami D DenOtter and Johanna Schubert. Hounsfield unit, 2019.
- [3] Sebastian Ruder. An overview of gradient descent optimization algorithms. *arXiv preprint arXiv:1609.04747*, 2016.

¹<https://creativecommons.org/licenses/by/4.0/>